Journal of Applied Polymer Science

Preparation, Structure, and Properties of End-Functionalized Miktoarms Star-Shaped Polybutadiene-Sn-Poly(styrene-butadiene) Rubber

Shuai Zhang,[1,2] Suhe Zhao,[1,2] Xingying Zhang,[2] Liqun Zhang,[1,2] Youping Wu[1,2]

[1]State Key Laboratory of Organic-Inorganic Composites, Beijing University of Chemical Technology, Beijing 100029, People's Republic of China

[2]Key Laboratory of Beijing City on Preparation and Processing of Novel Polymer Materials, Beijing 100029, People's Republic of China

Correspondence to: S. Zhao (zhaosh@mail.buct.edu.cn)

ABSTRACT: Two miktoarm star-shaped rubbers with large-volume functional groups of 1,1-diphenylhexyl at the ends of arms (DMS–PB–SBR) and one miktoarm star-shaped rubber with *n*-butyl groups at the ends of arms (BMS–PB–SBR) were prepared by 1,1-diphenylhexyllithium (DPHLi) and *n*-butyl lithium as initiators, respectively. The molecular structures and morphological properties of the three rubbers (MS–PB–SBR) were studied and compared with those acquired from the blend consisting of star-shaped solution-polymerized butadiene styrene rubber (S-SSBR) and butadiene rubber (PBR) prepared by ourselves. The results showed that MS–PB–SBR exhibited a more uniform distribution of PBR phase and a smaller phase size of PBR than that of S-SSBR/PBR blend. It is found that MS–PB–SBR composites filled with CB showed the lower Payne effect than that of S-SSBR/PBR/CB composite, suggesting that the MS–PB–SBR/CB composite (particularly the DMS–PB–SBR/CB composites) would possess excellent mechanical properties, high wet-skid resistance, and low rolling resistance. For the studied MS–PB–SBR systems, the contribution of large-volume functional groups at the end of PBR molecular chains to decrease the rolling resistance was larger than that of Sn coupling effect. It is envisioned that the miktoarm star-shaped rubbers with 1,1-diphenylhexyl groups at the molecular ends would be useful for making treads of green tires. © 2013 Wiley Periodicals, Inc. J. Appl. Polym. Sci. **2014**, *131*, 40002.

KEYWORDS: addition polymerization; elastomers; morphology; structure–property relations

Received 14 July 2013; accepted 23 September 2013

DOI: 10.1002/app.40002

INTRODUCTION

In recent years, in response to the rapid development of the automobile industry and the increasing shortage of oil resources, the requirements for high-performance automobile with high speed, safety, and energy-saving properties have been more urgent. It has been reported that the energy loss accounted for 30–40% of the total loss by car is used to overcome the rolling resistance of the tire, and 50% of the energy consumption by the tire is caused by the tire tread rolling resistance.[1] Therefore, reducing the tire tread rolling resistance is one of the effective steps to save energy. Nowadays, a lot of studies have been focused on the development of energy-saving green tire tread materials[2–6] by macromolecule design.[7,8]

Generally, rubbers with flexible chain and a high resilience have been considered to display low rolling resistance property, for example, butadiene rubbers. In addition, rubber materials with a coupled or passivated structure at the end of molecular chain also have low rolling resistance characteristic.[9] However, rubber materials with big pendant group have been considered to possess high wet-skid resistance, for instance, styrene–butadiene rubber. Consequently, it is very difficult to find one elastomer material exhibiting great balance between rolling resistance and wet-skid resistance properties.[10] To solve this problem, the traditional method is blending several kinds of rubbers with different structure to obtain a kind of material with good integration property, for example, the mixture of styrene–butadiene rubber and butadiene rubber.[11,12] Nevertheless, this method cannot well adjust the requirements of excellent comprehensive performance for tire tread as assumed because of existing difference in compatibility among different kinds of rubber.

The integral rubber concept was proposed by Nordesik[13] for preparing a tread material in 1984. However, this rubber with large molecular weight is difficult to be synthesized and processed thereafter. But this thought is very scientific and novel.

Table I. Structural Parameters of MS–PB–SBR

Compound no.	Mn (g/mol)	MWD	St[a] (%)	Bv[b] (%)	Total coupling efficiency (%)	Per-PBR[c] (%)	Per-SBR[d] (%)	PBR arm Mn (g/mol)	SBR arm Mn (g/mol)
B0	2,84,309	1.81	26.1	32.0	66.8	24.6	75.4	1,07,072	1,01,916
D1	2,84,324	1.64	26.9	32.6	60.8	14.6	85.4	1,31,144	90,869
D2	2,12,471	1.56	24.3	33.5	67.8	24.5	75.5	1,53,109	78,731

[a] Styrene content.
[b] The content of 1,2-butadiene structure.
[c] The percent rate of PBR in the coupled polymer.
[d] The percent rate of SBR in the coupled polymer.

Many investigators have done a large of works in this field. Zhang et al.[14,15] has adopted a new method that the three kinds of monomer are reacted meanwhile to form a new kind of random SIBR integral rubber with excellent property. Yan et al.[16] has used *n*-butyl lithium and $SnCl_4$ as initiator of anionic polymerization and coupling agent respectively to obtain star-shaped styrene–isoprene–butadiene random copolymer. Feng et al.[17,18] has investigated a novel tin-coupled star-shaped block copolymer (S-PB–PSB) by using anionic polymeric techniques. In short, different sequence and combination mode of the three kinds of monomer could prepare different integral rubber with good mechanical property, high antiskid properties and low rolling resistance. Thus, it has been considered that the rubber with integral performance could also be known as the integral rubber.

In this study, two kinds of miktoarms star-shaped rubber with 1,1-diphenylhexyl at the ends of arms (DMS–PB–SBR) and one kind of miktoarms star-shaped rubber with *n*-butyl at the ends of arms (BMS–PB–SBR) were prepared, respectively. The structure parameters of three samples were determined. The stress relaxation, mechanical properties, dynamic compression heat built-up, and dynamic mechanical properties of the two DMS–PB–SBR/CB, BMS–PB–SBR/CB and S-SSBR/PBR/CB composites was investigated. Morphological structures of the raw rubber samples and composites were observed by TEM. It is expected that our experimental results would be provide new insights for the design and synthesis of the tread material of green tires.

EXPERIMENTAL

Materials and Formulation

Materials. Cyclohexane (industrial grade), Styrene (St) (analysis grade), and alcohol (analysis grade) were all produced by Beijing Chemical Reagents Company (Beijing, China). Butadiene (Bd; polymerization grade) was provided by Beijing Yanshan Petrochemical Corporation (Beijing, China). Tetrahydrofuran (THF; analysis grade) was supplied by Beijing Chemical Works (Beijing, China). Functional organic lithium initiator named 1,1-diphenylhexyllithium (DPHLi)[19] was self-prepared.

Three miktoarms star-shaped rubber (B0, D1, and D2) were synthesized by living anion polymerization in our laboratory. The structural parameters for the three samples are shown in Table I, among which B0 was synthesized using Bu–Li initiator and other samples were synthesized using DPHLi initiator.

Polybutadiene (PBR) which was used for the blend (Y) was synthesized in our laboratory. Star-shaped SSBR (S-SSBR) was produced by Beijing Yanshan Petrochemical Co. (Beijing, China). Their structural parameters are listed in Table II. The mass ratio of PBR chains to SBR chains in MS–PB–SBR is 20/80, which is the same as that in Y.

CB (N234) was produced by Tianjin Haitun Carbon Black Co. (Tianjin, China); all other reagents, such as zinc oxide, sulfur, and so on, were commercial grade.

Formulation for Preparing the Rubber Compounds

Rubber: 100.0, N234: 50.0, Zinc oxide: 4.0, Stearic acid: 2.0, 2,2,4-trimethyl-1,2-dihydroquinoline: 1.5, *N*-cyclohexyl-2-benzothiazyl sulfenamide: 1.0, Tetramethylthiuramdisulfide: 0.2, Aromatic oil: 5.0, and Sulfur: 1.8 phr (Parts-per-hundred rubber).

Numbers of Sample

B0, D1, and D2 stand for three kinds of miktoarms star-shaped raw rubber, and Y stands for the S-SSBR/PBR blend.

B0c, D1c, and D2c stand for three kinds of miktoarms star-shaped rubber composites filled with CB, and Yc stands for the S-SSBR/PBR/CB composite.

Specimen Preparation

Preparation of Miktoarm Star-Shaped Rubber Samples. A 2-L stainless reactor and two 1-L glass reactors were purged by vacuumizing and transposition of nitrogen. The synthesis was

Table II. Structural Parameters of PBR and S-SSBR Used for the Blend Rubber

Compound no.	Mn (g/mol)	MWD	St[a] (%)	Bv[b] (%)	Total coupling efficiency (%)	Initiator
PBR	89,827	1.17	–	9.28	0	*n*-Butyl lithium
S-SSBR	3,13,000	1.59	23.7	37.5	100.0	Multifunctional lithium initiator[20]

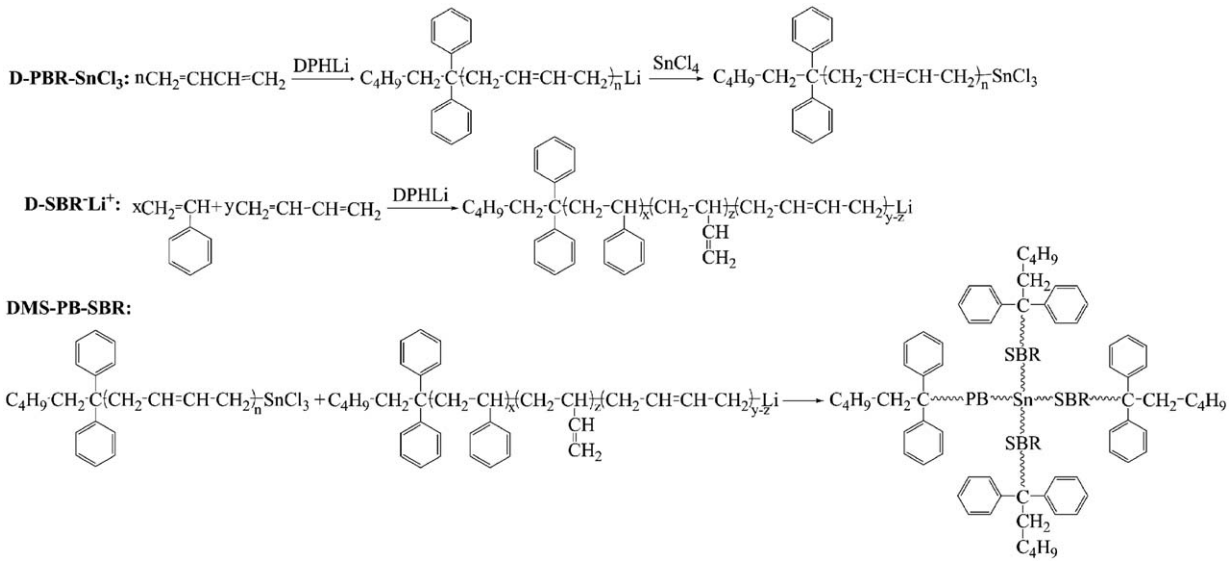

Figure 1. Scheme of DMS–PB–SBR polymerized reaction.

carried out in a three-stage procedure. The first stage was aimed to produce PBR^-Li^+ and SBR^-Li^+ in a 1-L glass reactor and the 2-L reactor, respectively. The polymerization was initiated by DPHLi or *n*-butyl lithium initiator. The polymerization temperature was kept at 50°C. The polymerization time for PBR^-Li^+ and SBR^-Li^+ was 2 and 1.5 h, respectively. Subsequently, in the second stage, PBR^-Li^+ solution was added into another 1-L glass reactor containing the same mole of $SnCl_4$ solution to form PBR–$SnCl_3$. In this process, the concentration of PBR^-Li^+ solution was very low, as well as in the process of reaction the PBR^-Li^+ solution was added slowly to the $SnCl_4$ solution under rapid stirring. In the last stage, according as the mass rate of PBR–$SnCl_3$/SBR^-Li^+ was 1 : 4, the PBR–$SnCl_3$ was added into SBR^-Li^+ solution. After reacting for 2 h, the polymer was purified by precipitation using alcohol and dried in a vacuum oven to constant weight. At last, the three kinds of samples (B0, D1, and D2), among which the end groups of molecular chain of D1 and D2 were 1,1-diphenylhexyl and that of B0 was *n*-butyl, were obtained.

The theoretic reaction mechanism of D1 and D2 samples is shown in Figure 1. Besides adopting *n*-butyl lithium initiator, the reaction mechanism of B0 sample is same as D1 and D2 samples.

Preparation of the Rubber Compounds

S-SSBR and PBR were mixed into blend by an open two-roll mill (Shanghai Rubber Machinery Works No. 1, Shanghai, China). After the mixtures were thin-passing and well-mixed, Carbon black (CB) and other addition agents were added into S-SSBR/PBR blend in turn for further mixing. Finally, the S-SSBR/PBR/CB compound was sheeted and waited for future use. The MS–PB–SBR/CB compounds were prepared in the same way.

Preparation of the Vulcanizates

The vulcanizing properties of the compounds were determined by a $P3555B_2$ Disc Vulkameter (Beijing Huanfeng Chemical Machinery Trial Plant, Beijing, China). An XLB-D350 × 350 plate vulcanization machine (Huzhou Dongfang Machinery Co., Zhejiang, China) was used to prepare the vulcanizates, and the curing condition was 150°C × t_{90} (optimum cure time).. The hydraulic pressure was 15 MPa and the thickness of vulcanizate sample was about 2 mm.

Structure–Morphology–Properties Measurement

The number-average molecular weight (M_n), weight-average molecular weight (M_w), polydispersity index (M_w/M_n) were measured by Waters 150-C gel permeation chromatograph, produced by Waters. The benzene abundance in coupled SBR and linear SBR was measured by ultraviolet absorption spectroscopy, produced by Waters. Tetrahydrofuran was used as the eluent at a flow rate of 1.0 mL/min at 30°C.

Stress relaxation was determined by RPA2000 Rubber Process Analyzer, produced by Alpha Technologies Co. The strain was 70%, the temperature was 100°C, the preheat time was 300 s and the test time was 120 s. The stress-relaxation time (i.e., the time needed for the stress to decrease to 36.8% of the initial stress under constant strain and temperature) was determined.

Dynamic mechanical property (strain sweep) was determined by RPA2000 Rubber Process Analyzer, produced by Alpha Technologies Co. The testing temperature was 60°C, the strain was varied from 0.28% to 42% and the frequency was 10 Hz.

Dynamic mechanical property (temperature sweep) was determined in a rectangular tension mode by VA3000 Dynamic Mechanical Thermal Analyzer, produced by 01dB-Metravib, France. Testing conditions: the temperature was from −80°C to 100°C, the speed of temperature rise was 3°C/min, the frequency was 10 Hz and the strain amplitude was 0.1%.

Mechanical properties were measured according to ASTM D638 at a tensile rate of 500 mm/min by CMT4104 Electrical Tensile Tester, produced by Shenzhen SANS Test Machine Co., China.

Shore A hardness and abrasion loss of vulcanizates were measured by an XY-1 rubber hardness apparatus (produced by 4th

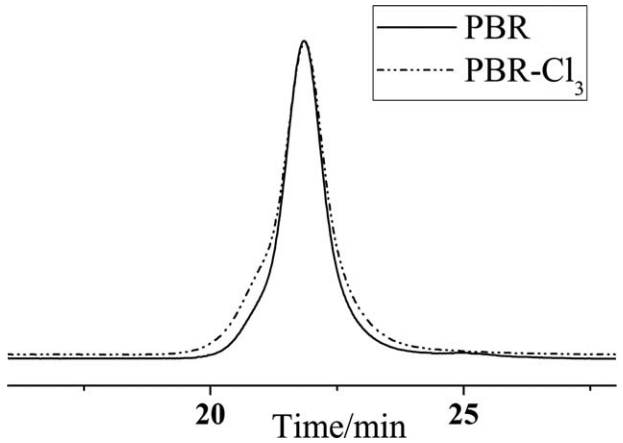

Figure 2. The GPC curve of D-PBR and D-PBR–$SnCl_3$ used in the synthesis of D1 sample.

Chemical Industry Machine Factory, Shanghai, China) and an MZ-4061 Akron-type abrasion testing machine with a rubber-wheel speed of 76 rpm (produced by Jiangsu Mingzhu Testing Machine Factory, Jiangsu, China), respectively.

Dynamic compression heat was determined by YS-25 Compression Heat Built-up Tester, produced by Shanghai rubber machinery works, China. Testing conditions: the preheating time was 25 min, the pre-heating temperature was 55°C, the compression time was 25 min, the frequency was 1800 min^{-1}, the stroke was 4.45 mm and the load was 1 MPa.

Morphological structure was observed by H-800-1 Transmission Electron Microscopy, produced by Hitachi Co., Japan. The acceleration voltage was 200 kV. The thin sections were cut by microtome under −100°C and collected on the copper grids. All the MS–PB–SBR samples and S-SSBR/PBR blend on copper grids were stained with OsO_4 vapor for 40 min.

RESULTS AND DISCUSSION

The Structure and Total Coupling Efficiency of Miktoarm Star-Shaped Rubber

Structural Characterization of D-PBR and D-PBR–$SnCl_3$. The GPC curves and molecular structure parameter of D-PBR (at the chain end of PBR with 1,1-diphenylhexyl) and D-PBR–$SnCl_3$ used in preparing D1 sample are shown in Figure 2 and Table III.

As seen from Figure 2 and Table III, there is almost no change between the molecular weights and their distribution (M_w/M_n). It illustrates that only one chloride in $SnCl_4$ react with living PBR^-Li^+ by using the appropriate way of feeding. In this way, the intermediate product D-PBR–$SnCl_3$ which has only one PBR chain in one miktoarms molecule could be obtained. GPC curves of the PBR chain and PBR–$SnCl_3$ used in preparing B0 and D2 are the same as those of the PBR chain and PBR–$SnCl_3$ used in preparing D1.

Table III. The M_n and M_w/M_n of D-PBR and D-PBR-$SnCl_3$

	D-PBR		D-PBR–$SnCl_3$	
Samples no.	M_n	M_w/M_n	M_n	M_w/M_n
D1	1,31,000	1.39	1,33,000	1.40

The Coupling Efficiency of Miktoarm Star-Shaped Rubber

The GPC–UV chromatogram of D1 sample is shown in Figure 3.

Figure 3(a) exhibits that the coupled and the residual linear molecular of D1 sample appear peaks separately. In this chart, peak 1 and peak 2 stand for coupled and linear polymer respectively. The ratio of peak 1's area to the sum of two peak's area could be the total coupling efficiency (E_T). In UV chromatogram [Figure 3 (b)], only SBR with benzene ring shows the absorption peak, and peak 1' and peak 2' stand for coupling and linear structure of SBR chain respectively, and the coupling efficiency of SBR chain (E_{SBR}) can also be calculated in the same way. The coupling efficiency of PBR (E_{PBR}) in MS–PBR–SBR sample can be worked out by considering experiment inventory. The formula of coupling efficiency is as follows:

$$E_{PBR} = \frac{M_T \times E_T - M_{SBR} \times E_{SBR}}{M_{PBR}} \quad (1)$$

M_T stands for the quality of the synthetic polymer (same as the experimental inventory); M_{SBR} and M_{PBR} stand for the inventory of living SBR^-Li^+ and PBR^-Li^+, respectively.

The percent rate of PBR and SBR in total coupling efficiency can be calculated by formula (2):

$$PerPBR = \frac{E_{PBR}}{E_{PBR} + 4 \times E_{SBR}} \quad (2)$$

All structure parameters are shown in Table I.

Morphological structure of MS–PB–SBR and S-SSBR/PBR blend

As shown clearly in Figure 4, four samples form the two-phase structure that consists of polybutadiene and styrene–butadiene random copolymer. The dark phase belongs to the domain of

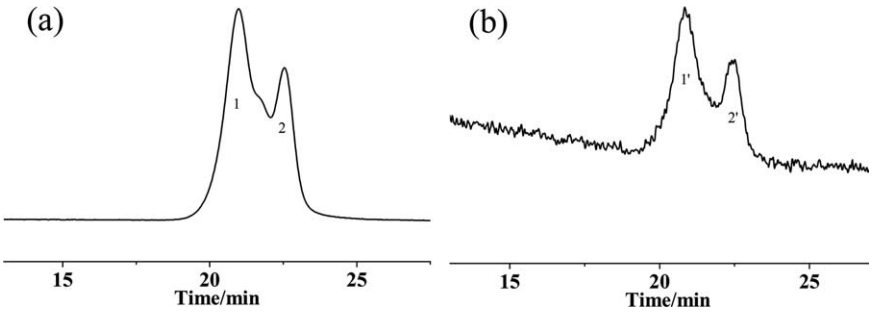

Figure 3. GPC and UV chromatogram of D1 sample: (a) GPC, (b) UV.

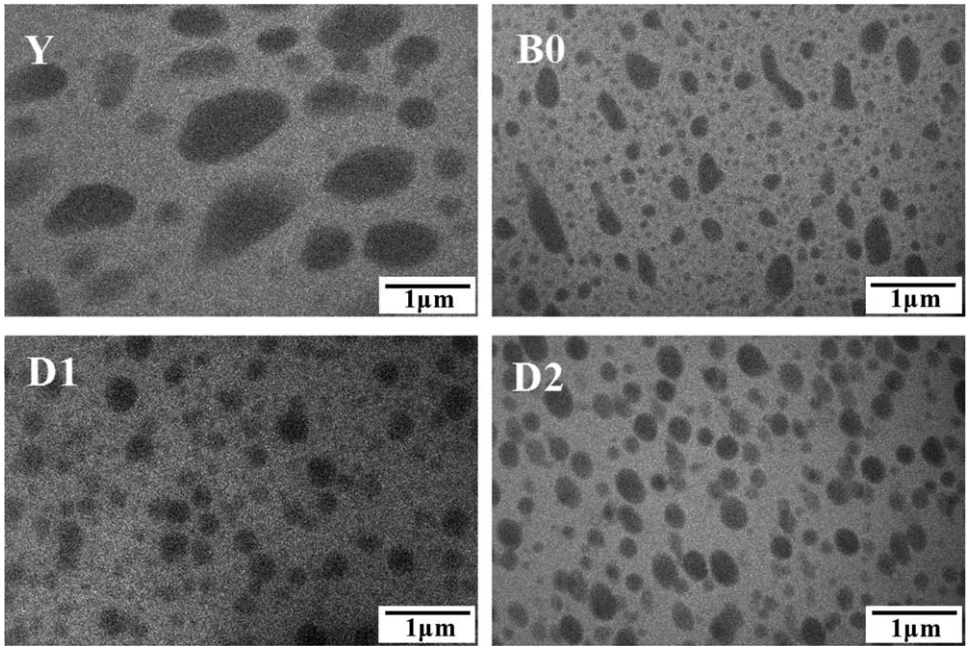

Figure 4. TEM photographs of MS–PB–SBR and S-SSBR/PBR blend (stained with OsO_4 for 40 min).

polybutadiene, and the gray light part formed continues phase is the domain of SBR random copolymers. The PBR phase size in Y is about 1 μm. However, the distribution of PBR phase in three MS–PB–SBR samples is more uniformity and PBR phase size is smaller, about 0.2–0.4 μm. This is because some PBR and SBR chains in MS–PB–SBR are connected by $SnCl_4$ to spur PBR phase to disperse uniformity. Among the three MS–PB–SBR samples, D2 has the best phase uniformity.

Stress Relaxation

As seen from Figure 5 and Table IV, the stress-relaxation time of D1c and D2c are longer than that of B0c. It is proved that the free movement of the molecular chain ends with 1,1-diphenylhexyl is restrained. The stress-relaxation rate of Yc is slightly longer than that of B0c due to linear structure of PBR and large molecular weight of S-SSBR in blend.

Dynamic Mechanical Properties

Strain-Sweep Spectra

Figure 6(a) shows that the decreasing amplitude ($\Delta G'$) of G' with increasing strain (ε%) is in order Yc > B0c > D1c > D2c in the test strain range (0.28–42%). This order indicates that the Payne effect[21,22] of Yc is the highest, which illustrates that CB disperses better in MS–PB–SBR than that in S-SSBR/PBR blend. This may be because the distribution of PBR phase in MS–PB–SBR is more homogeneous and PBR phase size is smaller. The Payne effect of B0c is higher than that of D1c and D2c, which reveals that 1,1-diphenylhexyl at the end of DMS–PB–SBR molecular chains could enhance the adsorption for CB particles and improve CB dispersion in the rubber matrix.

Figure 6(b) displays that the tan δ value of Yc increases with increasing ε% and presents an obvious peak at about 10% strain, while B0c and D1c present low peaks and D2c presents no peak. This may be because large CB aggregates in Yc composites are easy to breakdown at high strain, leading to the high tan δ. Due to good CB dispersion in D2c, the internal friction loss peak caused by the breakdown of CB aggregates disappears.

As we can see from Table I, the number of free PBR chain in D1 is more than that of B0. However, tan δ of D1c is smaller than that of B0c in the same strain, which illustrates that 1,1-diphenylhexyl at the end of molecular chains immobilize mobility of the free chain terminals and reduce the friction loss of the chain terminals,[23] and shows that the contribution of large-volume functional groups at the end of PBR molecular chains to decreasing rolling resistance is larger than that of Sn coupling effect. The tan δ of DMS–PB–SBR/CB composites presents D2c < D1c under the same strain due to the fact of that the total coupling efficiency of D2 is higher than that of D1.

Temperature-Sweep Spectra. It is reported that in the tire industry[24,25] tan δ value of the tread rubber at 0°C represents its wet-skid resistance and tan δ value of tread rubber at 60°C

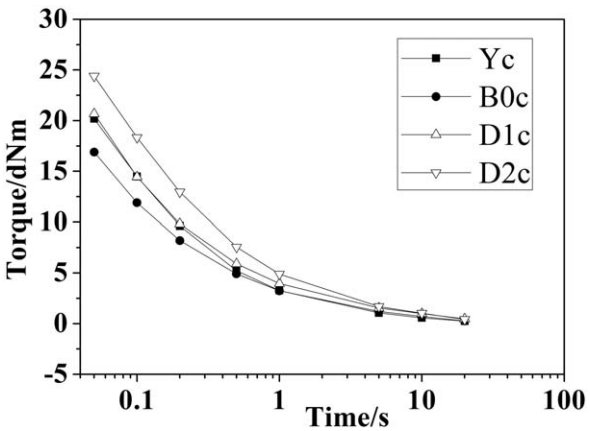

Figure 5. The stress-relaxation curves of four compounds.

Table IV. The Stress-Relaxation Time of Four Compounds

Compound no.	Yc	B0c	D1c	D2c
Stress-relaxation time/s	0.064	0.058	0.068	0.085

Table V. Tan δ of Four Vulcanizates

Compound no.	Yc	B0c	D1c	D2c
tan δ (0°C)	0.1707	0.2891	0.3116	0.1866
tan δ (60°C)	0.1103	0.1121	0.1022	0.0731

represents its rolling resistance. Therefore, the high performance tire tread material should have higher tan δ at 0°C and lower tan δ at 60°C.[26,27] The temperature (T) dependence of the storage modulus (E') and tan δ of four composites at a constant frequency are shown in Figure 7 and Table V.

It is seen from Figure 7(a) that the E' values of the four kinds of composites are similar in the glassy state, and the E' of S-SSBR/PBR/CB composite is distinctly higher than that of MS–PB–SBR/CB composites in the high-elastic state. At low strains ($\leq$0.1%), E' of the vulcanizate in the high-elastic state can be used as an index to evaluate filler–filler interaction. A high E' indicates that there are many filler aggregates[28] induced by the strong filler–filler interaction,[29] and it is consistent with the results of strain scanning in Figure 6(a).

From Figure 7(b) and Table V, tanδ at 0°C of three MS–PB–SBR/CB composites is markedly higher than that of Yc, which indicates that MS–PB–SBR/CB composites have high wet-skid resistance. Tan δ at 60°C of D1c and D2c is lower than those of Yc and B0c, which indicates that DMS–PB–SBR synthetized by DPHLi have low rolling resistance. Moreover, tanδ at 60°C of D2c is obvious lower than that of D1c. This is related to the higher total coupling efficiency, Per-PBR and lower slightly St% content of D2 are than those of D1.

TEM Photographs of Four Composites

As shown clearly in Figure 8, CB particles in Yc form obvious filler-network structure and 100–200 nm agglomeration phenomenon, because the distribution of PBR phase in Y is inhomogeneous and its size is large. The dispersion of CB in three kinds of MS–PB–SBR has been improved obviously, which demonstrates that miktoarms structure rubber possessed homogeneous phase structure could enhance the dispersion of CB. As for the dispersion of CB in the three MS-PB-SBR samples, D1 and D2 are better than B0, and especially the CB particle in D2 exhibits bead-chain (with 20–30 nm) distribution. The results further reveal that DMS–PB–SBR initiated by DPHLi has the strong adsorption for CB, which could efficiently make nano-fillers implement nano-dispersion in the matrix.

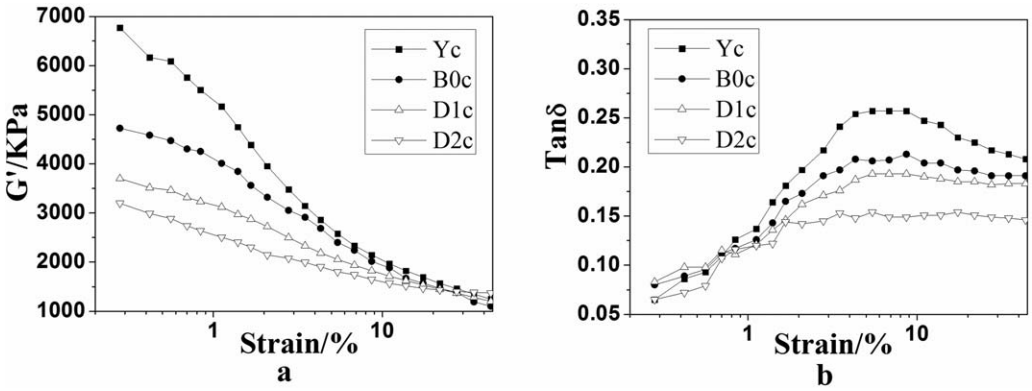

Figure 6. G' versus ε and tan δ versus ε curves of four composites.

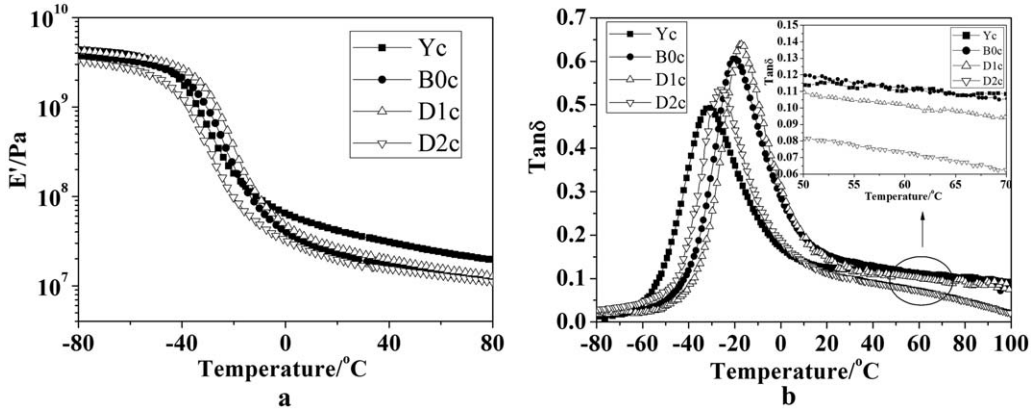

Figure 7. E' versus T and tan δ versus T curves of four composites.

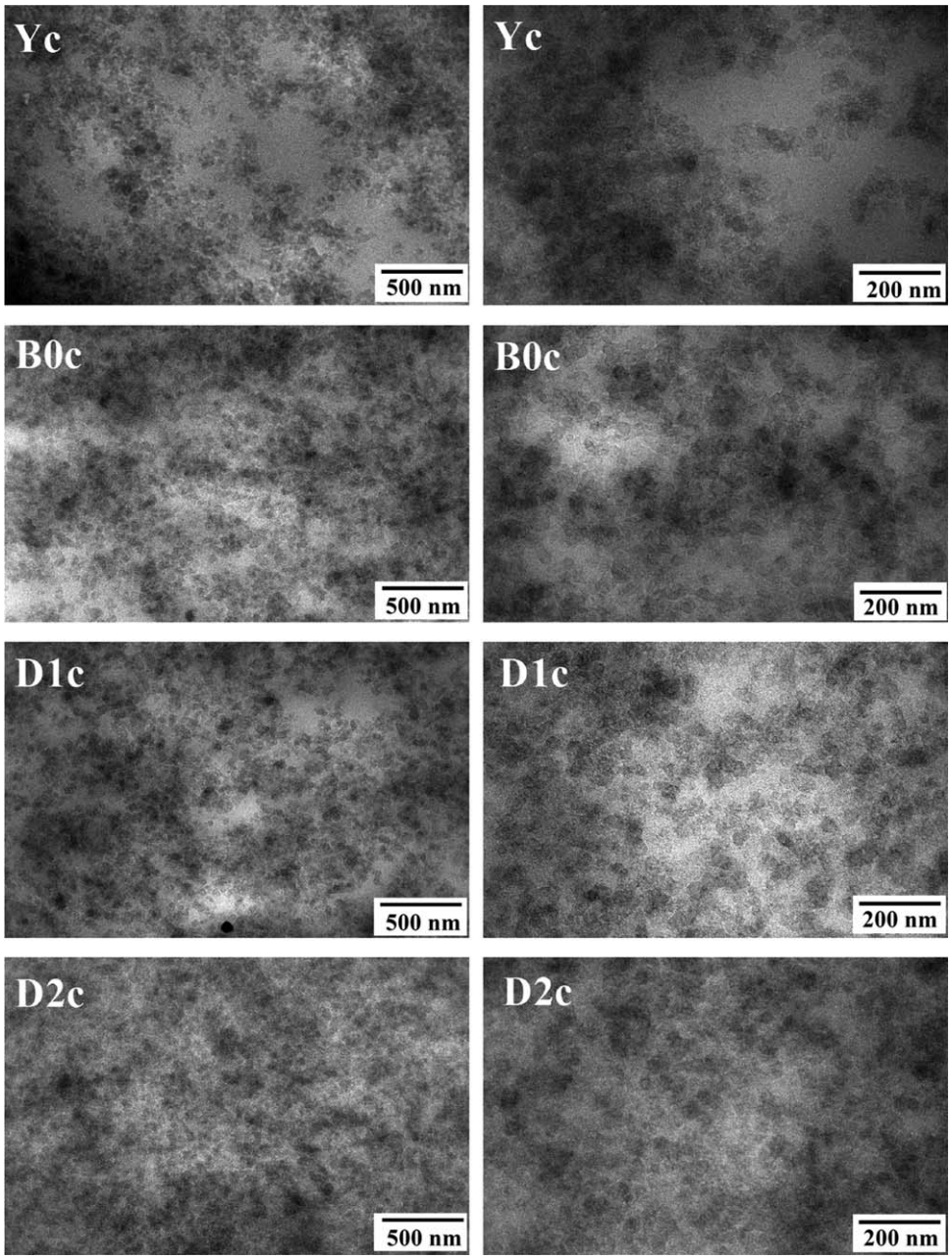

Figure 8. TEM photographs of four composites.

Table VI. Vulcanizing and Mechanical Properties of Four Composites Filled with CB

Compound no.	Yc	B0c	D1c	D2c
t_{10} (m:s)	5:03	5:45	5:53	5:47
t_{90} (m:s)	8:22	9:41	10:36	9:10
Shore A hardness	78	75	75	74
Tensile strength (MPa)	18.9	18.6	19.0	19.5
Modulus at 300% (MPa)	14.1	13.6	13.9	14.3
Elongation at break (%)	351	378	395	397
Permanent set (%)	8	8	6	8
Tear strength (kN m^{-1})	53.7	57.3	58.0	59.5
Abrasion loss (cm^{-3}/1.61 km)	0.1467	0.0829	0.0791	0.0972
Compression heat build-up (°C)	18.3	18.1	17.5	15.6
Compression permanent set (%)	3.21	2.56	2.18	1.63

Vulcanizing and Mechanical Properties

As seen from Table VI, the scorch time (t_{10}) and optimum cure time (t_{90}) of three kinds of composites, B0c, D1c, and D2c, are longer than that of Yc composite, which illustrates that miktoarms star-shaped structure could improve vulcanization security. The hardness of Yc is the highest due to the poor CB dispersion. Compared with Yc, the tear strength and elongation at break of three MS–PB–SBR/CB composites are high and the abrasion loss of three composites are significantly low, which is related to the better CB dispersion and the uniform distribution of PBR phase. The compression heat build-up and the compression permanent set of MS–PB–SBR/CB composites are smaller than that of Yc, which is consistent with the conclusion obtained from strain scanning in Figure 6(b).

Among the three kinds of MS–PB–SBR/CB composites, the tensile strength, elongation at break, tear strength, and modulus at 300% of D1c and D2c are bigger than that of B0c, which illustrates that the remarkable immobilization of chain ends creates a greater degree of orientation in the force field. The compression heat build-up of D1c and D2c are lower than that of B0c, which is consistent with the lower internal friction of DMS–PB–SBR/CB composites. Moreover, the compression heat build-up of D2c is obvious lower than that of D1c, consistent with the conclusion obtained above.

CONCLUSIONS

A new kind of integral rubber (miktoarms star-shaped rubber) was prepared by living anionic polymerization and special way of feeding. Meanwhile, the total coupling efficiency of miktoarms star-shaped rubber and the percent rate of PBR and SBR arm in the coupled molecule were calculated reasonably. The distribution of PBR phase in MS–PB–SBR matrix is more homogeneous and the PBR phase size is smaller than S-SSBR/PBR blend.

The stress-relaxation time of both DMS–PB–SBR/CB compound is longer than those of BMS–PB–SBR/CB and S-SSBR/PBR/CB compounds, which shows that molecular chain ended with 1,1-diphenylhexyl could restrain the free movement of macromolecular chain.

Despite the fact that the amount of PBR ended with 1,1-diphenylhexyl coupled to DMS–PB–SBR (D1 sample) was smaller than that of PBR ended with *n*-butyl coupled to BMS–PB–SBR (B0 sample), low rolling resistance of D1c sample was remarkable, which indicates that for MS–PB–SBR system studied the contribution of large-volume functional groups at the end of PBR molecular chains to decreasing rolling resistance is larger than that of Sn coupling effect.

Two DMS–PB–SBR/CB composites (D1c and D2c) present low hardness and compression heat build-up, low Payne effect, high tensile strength, elongation at break, tear strength and abrasion resistance. The results demonstrate that miktoarms star-shaped rubber with 1,1-diphenylhexyl groups at the end of molecular chains have integral performance required by the tire tread of green tires.

ACKNOWLEDGMENTS

The authors gratefully acknowledge financial supports from the Tenth five-Year Plan of China (2004 BA 310 A 41) and the Natural Science Foundation of China (50573005).

REFERENCES

1. Saito, Y.; Kobe, Y. *Kaut. Gummi. Kunstst.* **1986**, *39*, 30.
2. Castellano, M.; Conzatti, L.; Costa, G.; Falqui, L.; Turturro, A.; Valenti, B.; Negroni, F. *Polymer* **2005**, *46*, 695.
3. Liu, X.; Zhao, S. H. *J. Appl. Polym. Sci.* **2008**, *108*, 3038.
4. Bond, R.; Morton, G. F. *Polymer* **1984**, *25*, 132.
5. Mosnácek, J; Yoon, J. A.; Juhari, A.; Koynov, K.; Matyjaszewski, K. *Polymer* **2009**, *50*, 2087.
6. Li, H.; Sun, J.; Song, Y. H.; Zheng, Q. *J. Mater. Sci.* **2009**, *44*, 1881.
7. Passaglia, E.; Donati, F. *Polymer*, **2007**, *48*, 35.
8. Halasa, A. F.; Prentis, J.; Hsu, B.; Jasiunas, C. *Polymer* **2005**, *46*, 4166.
9. Wang, L.; Zhao, S. H.; Li, A.; Zhang, X. Y. *Polymer* **2010**, *51*, 2084.
10. Wang, M. J.; Sharon, X. L.; Mahmud, K. *J. Polym. Sci. Part B. Polym. Phys.* **2000**, *38*, 1240.
11. Hsu, W. L.; Halasa, A. F.; Matrana, B. A. *US Pat.* 5,422,403, 1995.
12. Halasa, A. F.; Hsu, W. L.; Zanzig, D. J. *US Pat.* 5,534,592, 1996.
13. Nordesik, K. H. *Kaut. Gummi. Kunstst.* **1985**, *38*, 178.
14. Zhang, H.; Zhang, X. Y.; Cheng, J.; Jin, G. T. *China Elastomer.* **1997**, *7*, 34.
15. Zhang, H.; Zhang, X. Y.; Cheng, J.; Jin, G. T. *China Elastomer.* **1997**, *7*, 44.
16. Yan, Z. L.; Jin, G. T. *China Rubber Ind.* **2000**, *47*, 662.
17. Feng, H. D.; Zhang, X. Y.; Zhao, S. H. *J. Appl. Polym. Sci.* **2009**, *110*, 228.
18. Feng, H. D.; Zhang, X. Y.; Zhao, S. H. *J. Appl. Polym. Sci.* **2009**, *111*, 602.
19. Zhang, X. Y.; Chen, B.; Zhao, S. H.; Bai, Y.; Xu, L. M. *Can Pat.* 201010618277.2, 2010.
20. Bai, Y.; Zhao, S. H.; Tong, Y. Y.; Zhang, X. Y.; Liu, X.; Tian, M. *J. Appl. Polym. Sci.* **2013**, *128*, 2516.
21. Payne, A. R. *J. Appl. Polym. Sci.* **1962**, *6*, 57.
22. Payne, A. R.; Whittaker, R. E. *Rubber Chem. Technol.* **1971**, *44*, 440.
23. Sarva, S. S.; Hsieh, A. J. *Polymer* **2009**, *50*, 3007.
24. Zeng, Z. Q.; Yu, H. P.; Wang, Q. F.; Lu, G. *J. Appl. Polym. Sci.* **2008**, *109*, 1944.
25. Takino, H.; Nakayama, R.; Yamada, Y.; Kohjiya, S.; Matsuo, T. *Rubber Chem. Technol.* **1997**, *70*, 584.
26. Lu, J. M.; Zhang, X. Y.; Zhao, S. H.; Yang, W. T. *J. Appl. Polym. Sci.* **2007**, *104*, 3917.
27. Lu, J. M.; Zhang, X. Y.; Zhao, S. H.; Yang, W. T. *J. Appl. Polym. Sci.* **2007**, *104*, 3924
28. Evans, L. R.; Fultz, W. C.; Huber, J. M. *Rubber World.* **1998**, *219*, 38.
29. Aso, O.; Eguiazábal, J. I.; Nazábal, J. *Compos. Sci. Technol.* **2007**, *67*, 2854.